

Koba-Nielsen-Olesen scaling, its violation, and the structure of hadrons

Serge Rudaz

School of Physics and Astronomy, University of Minnesota, Minneapolis, Minnesota 55455

Pierre Valin

Department of Physics, McGill University, Montreal, Quebec, Canada H3A 2T8

(Received 26 June 1985)

We revive a quark-parton model of multiparticle production in which Koba-Nielsen-Olesen (KNO) scaling at energies up to the CERN ISR results from the Bjorken scaling of quark longitudinal-momentum distribution functions in hadrons. KNO-scaling violation in total inclusive data at and above ISR energies is ascribed to the onset of gluon-gluon collisions as a new (rising) component of the total inelastic cross section. A new multiplicity formula is obtained, and excellent agreement is obtained for the KNO function and all moments of multiplicity distributions up to CERN $Spp\bar{S}$ Collider energies. Tentative predictions for the Fermilab Tevatron Collider and Superconducting Super Collider energy ranges are presented, and the uncertainties of such extrapolations discussed. We also discuss the question of KNO-scaling violation in non-single-diffractive as opposed to total inclusive data.

I. INTRODUCTION

The discovery of clear two-jet events at the CERN $Spp\bar{S}$ Collider¹ has recently provided brilliant confirmation of the QCD parton picture of hard hadron collision processes at the very large momentum transfers ($Q^2 \sim 10^3 \text{ GeV}^2$) where perturbative QCD is expected to provide a reliable description of the underlying constituent scattering. Jet angular distributions are well described in the parton c.m. frame by an expression of the form

$$\frac{d\sigma}{dx_1 dx_2 d\cos\theta} = \sum_{i,j} f_i(x_1) f_j(x_2) \frac{d\hat{\sigma}_{ij}}{d\cos\theta}, \quad (1.1)$$

where the sum runs over parton species, $f_i(x)$ is the probability of finding a constituent i of the proton with longitudinal-momentum fraction x at the appropriate large Q^2 , and the caret denotes the parton-parton differential scattering cross section.

This remarkable success of the QCD parton model in describing hard-scattering processes in very-high-energy hadron collisions is indeed gratifying, but should not obscure the fact that such processes actually comprise a tiny fraction of the total $p\bar{p}$ cross section. The remaining, overwhelming fraction of the $p\bar{p}$ events corresponds to low-momentum-transfer processes, where perturbative QCD is inapplicable. In the description of such processes, we must rely on phenomenology, which may or may not be closely inspired by soft QCD folklore.

Clearly, somehow, the bulk of the hadron collision cross section should reflect the internal structure of hadrons, and, in fact, parton models of low-momentum-transfer processes have met with a measure of phenomenological success.² Most important is the success of the additive quark model³ in predicting ratios of cross sections: the prediction³ $\sigma(\pi p)/\sigma(pp) = \frac{2}{3}$ of the additive quark model is well verified over the entire energy range

for which data is available, i.e., up to the end of the CERN ISR energy range where we encounter the rise of the total pp cross section [experimentally, in fact, $\sigma(\pi p)/\sigma(pp) \simeq \frac{3}{5}$]. The explanation of this success of the additive quark model is possibly the most important question to be addressed by a future theory of soft QCD.

Another interesting result is due to Goldberg⁴ who suggested that the relatively fast decrease of the Feynman- x spectra of mesons in the proton fragmentation region be a reflection of the valence-quark structure functions of the initial proton: the x distribution of a pion in the fragmentation region is expected to reflect that of a valence quark which it shares with the incoming proton. Hence with

$$F^{p \rightarrow h}(x) = \frac{x}{\sigma} \frac{d\sigma^{p \rightarrow h}}{dx},$$

we have

$$F^{p \rightarrow \pi^+}(x) \propto u_p(x) \quad (1.2)$$

and

$$\frac{F^{p \rightarrow \pi^-}(x)}{F^{p \rightarrow \pi^+}(x)} = \frac{d_p(x)}{u_p(x)}, \quad (1.3)$$

both predictions in excellent accord with experiment^{2,5} [where $q_p(x)$ is the valence structure function of the quark q in the proton].

In this paper, in the spirit of the additive quark model, we develop a parton model for multiplicity distributions of hadrons produced in high-energy pp and $p\bar{p}$ collisions. The basic idea was outlined more than a decade ago by Eilam and Gell,⁶ who showed that Koba-Nielsen-Olesen (KNO) scaling⁷ followed from the Bjorken scaling of quark structure functions in a parton model of multiparticle production, provided the total multiplicity grows as a power of s . Such behavior ($\propto s^{1/4}$) is in fact in good agreement with data up to ISR energies. In the interven-

ing years, the importance of the gluon content of the proton was established indirectly through the analysis of deep-inelastic lepton-proton collisions: gluons carry about half the proton momentum, although the gluon distribution is still very uncertain, especially at small x and Q^2 (note that this uncertainty has little effect on the small- x , large- Q^2 behavior of gluon distributions as calculated via the Altarelli-Parisi equations).

We shall assume that the total inelastic pp and $p\bar{p}$ cross sections reflect the presence of both quarks and gluons in the proton. In particular, we shall ascribe the rising part of the cross section to the onset of gluon-gluon processes, a suggestion made by many people over the years.⁸ Thus, we write at ISR energies and beyond

$$\sigma_{\text{inel}}(s) = \sigma_q + \sigma_g(s), \quad (1.4)$$

where σ_q is the part due to qq collisions at low (sub-ISR) energies where the additive-quark-model predictions for cross-section ratios are verified. The gluon part is assumed to grow as $\ln^2(s/s_0)$: the scale s_0 is a few hundred GeV^2 , and may perhaps be understood as corresponding to the onset of resonant glueball production.⁹ For example, we would expect a new threshold at

$$x_1 x_2 s = M_G^2, \quad (1.5)$$

where M_G is some glueball mass. With $\bar{x} \simeq \frac{1}{8}$, say, on the average and $M_G = 2 \text{ GeV}$, this suggests $s_0 \sim 200 \text{ GeV}^2$ or so. In fact, the average particle content of ISR and $Spp\bar{S}$ events seems to indicate¹⁰ a slow rise in the relative number of η mesons which could be dominant decay products of glueballs: this question deserves further experimental study.

The onset of a rising gluon-gluon inelastic cross section serves to explain the observed violation of KNO scaling seen in the total inclusive $Spp\bar{S}$ data.¹¹ Another important point is the energy dependence of the total charged multiplicity which is well fit by a simple $s^{1/4}$ form at low energies, which however does not successfully extend to collider energies. This effect is also explained in terms of the increasing importance of gluon-gluon processes, for which the available energy for particle production is on the average less than in a quark-quark collision, because the gluons are typically found at smaller x than valence quarks. A consequence of this picture is the expectation that the additive quark model of cross-section ratios is expected to fail at very high energies, due to the differing gluon contents of mesons and protons. This question can be investigated using a fixed-target setup at the Fermilab Tevatron and perhaps the Superconducting Super Collider (SSC).

In what follows, we shall make extensive use of quark and gluon distribution functions, and there is a question as to which average Q^2 is the appropriate one for soft hadron collisions. One often immediately thinks $Q^2 \sim \langle p_\perp \rangle^2 \sim (400 \text{ MeV})^2$, a rather small value which would seem to preclude the use of the parton model. In fact, the appropriate Q^2 can be somewhat larger, as demonstrated by Pokorski and Wolfram,¹² who proposed a simple, direct, empirical method for its determination. Suppose the c.m. momenta of the initial hadrons in a

high-energy collision are p_1 and p_2 so that the final hadronic systems have momenta $p_1 + Q$ and $p_2 - Q$. If we now assume (1) that $|Q| \ll \sqrt{s}$ and is at most slowly varying with \sqrt{s} (as suggested by the data), and (2) that on the average the various components of Q_μ are comparable (recall that in Feynman's parton picture of inelastic hadronic collisions¹³ the "wee" four-momentum exchange has a nonzero longitudinal component), then the invariant masses of the produced hadronic systems will be

$$M^2 \simeq 2p \cdot Q \simeq \sqrt{s} |Q|, \quad (1.6)$$

whereas M^2 can be directly calculated, say in the forward ($y > 0$) hemisphere, via

$$M^2 = E_{\text{tot}}^2 - P_{L\text{tot}}^2 \quad (1.7)$$

with

$$E_{\text{tot}} = \int \frac{dN}{d^2 p_\perp dy} d^2 p_\perp m_\perp \cosh y \, dy, \quad (1.8)$$

$$P_{L\text{tot}} = \int \frac{dN}{d^2 p_\perp dy} d^2 p_\perp m_\perp \sinh y \, dy, \quad (1.9)$$

and where the total transverse momentum vanishes by definition. The available rapidity range is $0 \leq y \leq Y/2$ with $Y = \ln(s/m_p^2)$ and the transverse mass $m_\perp = (\mu^2 + p_\perp^2)^{1/2} \simeq |p_\perp|$ for pions. With the reasonable approximation that the hadrons are produced fairly uniformly over most of the rapidity interval, we then get

$$E_{\text{tot}} \simeq \int d^2 p_\perp |p_\perp| \frac{dN}{d^2 p_\perp} h(y=0) \sinh(y/2) \simeq \sqrt{s}/2, \quad (1.10)$$

$$P_{L\text{tot}} \simeq \int d^2 p_\perp |p_\perp| \frac{dN}{d^2 p_\perp} h(y=0) [\cosh(y/2) - 1], \quad (1.11)$$

where $h(y=0)$ is the height of the rapidity "plateau," slowly rising with increasing \sqrt{s} . It is now simple to calculate M^2 from Eq. (1.7), with the result

$$M^2 \simeq h(y=0) \langle p_\perp \rangle \sqrt{s} \quad (1.12)$$

whence, comparing with Eq. (1.6), we get the empirical estimate

$$|Q| \simeq h(y=0) \langle p_\perp \rangle. \quad (1.13)$$

Both $h(y=0)$ and $\langle p_\perp \rangle$ are slowly increasing functions of \sqrt{s} and Eq. (1.13) indicates that, over a wide energy range, the appropriate $Q^2 \sim 1 \text{ GeV}^2$ hardly changes at all. This value may serve to justify the incoherence assumption underlying the additive quark model since, with the proton radius $R_p \sim 1 \text{ F}$, we get $QR_p > 1$. We also note that perturbative QCD violations of Bjorken scaling are irrelevant to parton models of soft hadronic processes. The result, Eq. (1.13), also suggests an interesting speculation: it may be possible to estimate the magnitude of the total pp and $p\bar{p}$ cross sections using a formula of the form (1.4) by calculating $\sigma_g(s)$ from (1.1) with the energy-dependent empirical minimum momentum transfer $|Q|$ in Eq. (1.13) to cut off the Coulomb divergence of the per-

turbative gluon-gluon cross section. This could serve to justify the phenomenological ansatz adopted by Gaisser and Halzen in Ref. 8.

The plan of this paper is then as follows. In Sec. II we review and expand on the Eilam-Gell model of KNO scaling, as relevant only up to energies where the pp total cross section begins to rise: only quark-quark collisions are relevant here, the motivation being the success of the additive quark model of cross-section ratios in that energy range. We obtain analytic expressions for the KNO-scaling function and for the dispersion $D_2 = (\langle n^2 \rangle - \langle n \rangle^2)^{1/2}$ which are found to be in excellent agreement with data up to Fermilab or CERN SPS energies: in particular, we derive the Wroblewski relation¹⁴ $D_2 \propto (\langle n \rangle - n_0)$, which works very well indeed.

In Sec. III the model is extended to include the effects of gluons as the origin of KNO-scaling violations seen at the high end of the ISR energy range and at the $Spp\bar{S}$ Collider. We also propose a new multiplicity formula which agrees well with data at all energies.¹⁵ Extrapolated to very high energies, this formula implies larger charged multiplicities than the conventional phenomenological fit

$$\langle n \rangle = a + b \ln s + c \ln^2 s .$$

Our considerations apply to the total inclusive inelastic data: we show that these data at different energies do not in fact imply a strong violation of KNO scaling. In Sec. IV we address the question of the effect of the removal of the so-called single-diffractive-dissociation events from the data [resulting in the so-called non-single-diffractive (NSD) sample]. We show how this somewhat arbitrary cut results in KNO distributions which exhibit much more KNO-scaling violation for a very simple reason, related to the behavior of the average charged multiplicity $\langle n \rangle$ for increasing c.m. energies.

In Sec. V we offer predictions for Super Collider energies (Tevatron Collider and SSC): these depend significantly on the choice of high-energy parametrization for $\sigma_{\text{tot}}(s)$. Section VI serves to summarize our results and conclusions.

II. KNO SCALING AND THE ADDITIVE QUARK MODEL UP TO ISR ENERGIES

In this section, we develop and extend the Eilam-Gell⁶ picture of KNO scaling in pp collisions at low (sub-ISR) c.m. energies, resulting from the Bjorken scaling of quark distribution functions in the framework of the additive quark model. We reiterate that, in this energy range, and motivated by the empirical success of the additive quark model for cross-section ratios, the inelastic cross section is attributed to only one quark-quark component.

The basic ansatz is similar in form to Eq. (1.1), namely,

$$\frac{1}{\sigma_{\text{inel}}} \frac{d\sigma_{\text{inel}}}{dx_1 dx_2} = A f(x_1) f(x_2) , \quad (2.1)$$

where A is a normalization constant to be fixed later, and $f(x)$ is the valence-quark distribution function (in what follows, we do not distinguish $u(x)$ from $d(x)$ for the

purpose of obtaining simple analytic formulas: we have also carried out the calculation with different u and d distribution functions, as will be discussed shortly). The energy available for particle production is simply the total parton c.m. energy

$$\hat{s} = x_1 x_2 s . \quad (2.2)$$

The remaining quarks, spectators in the incoming protons, are dressed by an unspecified mechanism related to confinement (string formation and breaking, etc.). Event by event, we assume a narrow multiplicity distribution for particles produced by the basic parton collision:

$$n' = k(x_1 x_2 s)^\alpha . \quad (2.3)$$

The reason for the prime in Eq. (2.3) is that one should also include the leading particle contribution to the charged multiplicity in a given event. To do this, we assume that the spectator quarks can be dressed by u or d quarks with equal probabilities $p/2$, or by a strange quark with probability $1-p$. It is not difficult to see that this leads to $\frac{2}{3} + p$ additional charged leading baryons. Note that this would also give $\Lambda^0/p = (1-p)/p$ which is experimentally found¹⁰ to be about $\frac{1}{3}$, so that $p \approx 0.7-0.8$. We shall accordingly take the number of charged particles produced in a given event to be

$$n = n' + n_0, \quad n_0 = 1.3 . \quad (2.4)$$

Our remaining considerations, e.g., in the derivation of the KNO-scaling function, always involve $n' = n - n_0$. It has in fact long been known¹⁶ that such an n' was a better variable for discussion of multiplicity distributions than simply n .

From the above, we write

$$P_n = \frac{\sigma_n}{\sigma_{\text{inel}}} = \frac{1}{\sigma_{\text{inel}}} \frac{d\sigma_{\text{inel}}}{dn} = A \int dx_1 dx_2 f(x_1) f(x_2) \delta(n' - k(x_1 x_2 s)^\alpha) . \quad (2.5)$$

Note the δ function, narrowest of all distributions, essential to the derivation of KNO scaling which follows, as we will explain. From (2.5) we get, by integration over x_2 ,

$$P_n = \frac{A}{k\alpha s} \int \frac{dx_1}{x_1} \left[\frac{n'}{k} \right]^{1/\alpha-1} f(x_1) \times f((n'/k)^{1/\alpha}/x_1 s) . \quad (2.6)$$

Now note that

$$\begin{aligned} \langle n \rangle &= \frac{\int dn n P_n}{\int dn P_n} \\ &= n_0 + \frac{\int dx_1 dx_2 k(x_1 x_2 s)^\alpha f(x_1) f(x_2)}{\int dx_1 dx_2 f(x_1) f(x_2)} \end{aligned} \quad (2.7)$$

that is

$$\langle n \rangle = \langle n' \rangle + n_0, \quad \langle n' \rangle = k s^\alpha \langle x^\alpha \rangle^2 \quad (2.8)$$

with

$$\langle x^\alpha \rangle = \frac{\int_0^1 dx x^\alpha f(x)}{\int_0^1 dx f(x)}. \quad (2.9)$$

From (2.8) we have

$$k^{1/\alpha_S} = \langle n' \rangle^{1/\alpha} / \langle x^\alpha \rangle^{2/\alpha} \quad (2.10)$$

and so

$$\begin{aligned} P_n &= \frac{A}{k\alpha_S} \int \frac{dx}{x} f(x) f((n'/\langle n' \rangle)^{1/\alpha} \langle x^\alpha \rangle^{2/\alpha} / x) \\ &\quad \times \left[\frac{n'}{k} \right]^{1/\alpha-1} \\ &= \frac{A}{\alpha \langle n' \rangle} \int \frac{dx}{x} f(x) f(\rho^{1/\alpha} / x) \rho^{1/\alpha-1} \langle x^\alpha \rangle^2, \end{aligned} \quad (2.11)$$

where we have defined

$$\rho = z' \langle x^\alpha \rangle^2, \quad (2.12)$$

$$z' = n' / \langle n' \rangle. \quad (2.13)$$

Finally we obtain the KNO-scaling form⁶

$$\begin{aligned} \psi(z') \equiv \langle n' \rangle P_n &= \frac{A}{\alpha} \rho^{1/\alpha-1} \langle x^\alpha \rangle^2 \\ &\quad \times \int_{\rho^{1/\alpha}}^1 \frac{dx}{x} f(x) f(\rho^{1/\alpha} / x). \end{aligned} \quad (2.14)$$

Note that when $x_1 = x_2 = 1$,

$$\left. \frac{n'}{\langle n' \rangle} \right|_{\max} = \frac{k_S \alpha}{k_S \alpha \langle x^\alpha \rangle^2} = \frac{1}{\langle x^\alpha \rangle^2} \equiv k \quad (2.15)$$

so in fact

$$\rho = z' / z'_{\max} = z' / k. \quad (2.16)$$

The lower limit of integration in Eq. (2.14) follows from the fact that $\rho^{1/\alpha} / x \leq 1$ for the formalism to make sense. Note also that, in order to have a nonsingular behavior of $\psi(z')$ as $z' \rightarrow 0$, it is required that if $f(x)$ is of the form $x^{-q}(1-x)^p$, then $q < 1 - \alpha$. This also ensures that $\langle x^\alpha \rangle$ is finite, which is also clearly necessary. At this point, we see why the δ function in Eq. (2.5) is crucial to the derivation of KNO scaling, namely, that ψ is a function of $n' / \langle n' \rangle$: any other choice (e.g., a Gaussian of width ξ) would introduce a new parameter with which to form another ratio n' / ξ , thus violating KNO scaling.

Lastly, the normalization A is fixed via the conventional normalization of the KNO-scaling function

$$\int dz' \psi(z') = \int dz' z' \psi(z') = 2 \quad (2.17)$$

which yields

$$A = 2 / \left[\int dx f(x) \right]^2. \quad (2.18)$$

Equations (2.14) and (2.18) completely determine the KNO-scaling curve once α is fixed [From Eq. (2.8) and data] and $f(x)$ is known.

At this point, we note that $\langle n \rangle \sim s^{1/4}$ is known to give an excellent fit to low-energy multiplicity data: in the fol-

lowing, we shall accordingly choose $\alpha = \frac{1}{4}$. This in no way commits us to the Landau hydrodynamic model. In fact, such a power law can easily arise from the following very simple picture (necessarily nonperturbative) of qq hadronic system decay. Consider an initial "fireball" of invariant mass W , which splits into two systems (e.g., as favored in the framework of the $1/N$ expansion), each of invariant mass $W_1 = W/c$, where c is a fixed number. Let the process continue, resulting in a tree, until L steps have occurred. At the final step, $W_L = W/c^L = W_0$, where W_0 is some minimum resonance mass. Then the final multiplicity is

$$n \sim 2^L \quad (2.19)$$

with

$$L = \frac{1}{\ln c} \ln \left[\frac{W}{W_0} \right] \quad (2.20)$$

so that

$$n \sim \left[\frac{W}{W_0} \right]^{\ln 2 / \ln c}. \quad (2.21)$$

If $c = 4$, for example,

$$n \sim W^{1/2} \sim s^{1/4}. \quad (2.22)$$

This is an old argument (see, e.g., Polyakov¹⁷ in a completely different context) and shows that a power-law behavior for the multiplicity is perfectly reasonable. It is not however obtained from the perturbative QCD jet calculus.

A closed analytic form for $\psi(z')$ is easily obtained with the following naive choice for the valence-quark distribution:

$$f(x) = \frac{N_v}{\sqrt{x}} (1-x)^3, \quad (2.23)$$

where N_v is a normalization constant. Using Eqs. (2.14), (2.15), and (2.18), the result is

$$\begin{aligned} \psi(z') &= \frac{2450}{1089} \rho \left\{ \frac{11}{3} (\rho^{12} - 1) + 9\rho^4 (\rho^4 - 1) \right. \\ &\quad \left. - 4 \ln \rho [\rho^{12} + 1 + 9\rho^4 (\rho^4 + 1)] \right\}, \end{aligned} \quad (2.24)$$

where we recall that $\rho = z' / K$. The normalization factors are easily calculated. For example, $\langle x^{1/4} \rangle$ is given in terms of Euler beta functions as the ratio

$$\langle x^{1/4} \rangle = \frac{B(\frac{3}{4}, 4)}{B(\frac{1}{2}, 4)} = \frac{(\frac{1}{2})_4}{(\frac{3}{4})_4} = \frac{(\frac{1}{2})_{1/4}}{(\frac{9}{2})_{1/4}}, \quad (2.25)$$

where the Pochhammer symbol $(q)_a$ is defined¹⁸

$$(q)_a = \frac{\Gamma(q+a)}{\Gamma(q)}. \quad (2.26)$$

In fact one easily finds $\langle x^{1/4} \rangle = \frac{16}{33}$ whence

$$K = \langle x^{1/4} \rangle^{-2} = \frac{1089}{256}, \quad (2.27)$$

i.e.,

$$z'_{\max} \simeq 4.25 \quad (2.28)$$

in this case. The overall normalization factor in Eq. (2.24) follows similarly from the definition (2.18).

We show in Figs. 1(a) and 1(b) (on a linear and semilogarithmic plot, respectively) a comparison of the analytic formula (2.24) with a compilation¹⁹ of total inclusive (i.e., including the so-called single-diffractive component) Serpukhov and Fermilab data. Also shown, as a dotted curve, is the result which follows from the numerical integration of Eq. (2.14) using the valence quark distributions (at low Q^2) given by Eichten, Hinchliffe, Lane, and Quigg.²⁰ We see that the agreement with the data is excellent. The difference between the two curves can serve as an estimate of the theoretical uncertainty in the practical application of Eq. (2.14). Note that this model does not distinguish “diffractive” and “nondiffractive” events. In fact, it is most naturally applied to the total inclusive inelastic data, with no “single-diffractive” subtractions. We will return to this point in Sec. IV.

Note that the relatively baroque form, Eq. (2.24), is quite different from the various formulas proposed to date in the literature (see, e.g., the reviews listed in Ref. 21). It is remarkably successful to highest Fermilab energies, and contains no free parameter, once the power law of the

multiplicity and the form of the valence-quark distribution function are fixed from other considerations. In fact, the shape of the KNO-scaling function obtained in this way is quite sensitive to the behavior of $f_q(x)$ near $x=0$ and 1. Any choice other than the naive one [Eq. (2.23)] will usually fail to reproduce the data shown in Figs. 1(a) and 1(b). The fact that the quark distribution function obtained from deep-inelastic scattering can be used here in the description of largely low- p_\perp phenomena can be understood on the basis of the Pokorski-Wolfram¹² estimate of the typical momentum transfer in “soft” hadronic collisions $|Q| \sim h(y=0)\langle p_\perp \rangle$ (reviewed in Sec. I above), which shows that $\langle p_\perp \rangle$ is *not* the appropriate scale, and which justifies the incoherence assumption used here as well. These considerations serve to highlight the distinction between the picture of hadronic collisions presented here, and that of the proponents of the dual parton model (see, e.g., Ref. 22) who argue that the appropriate power of $(1-x)$ to be used for valence quark distributions should be 1.5. There, this smaller power reflects the crucial role played by diquark systems in the formation of a chain, whose breakup involves $q\bar{q}$ pairs from the sea, with the final state described quantitatively using fragmenta-

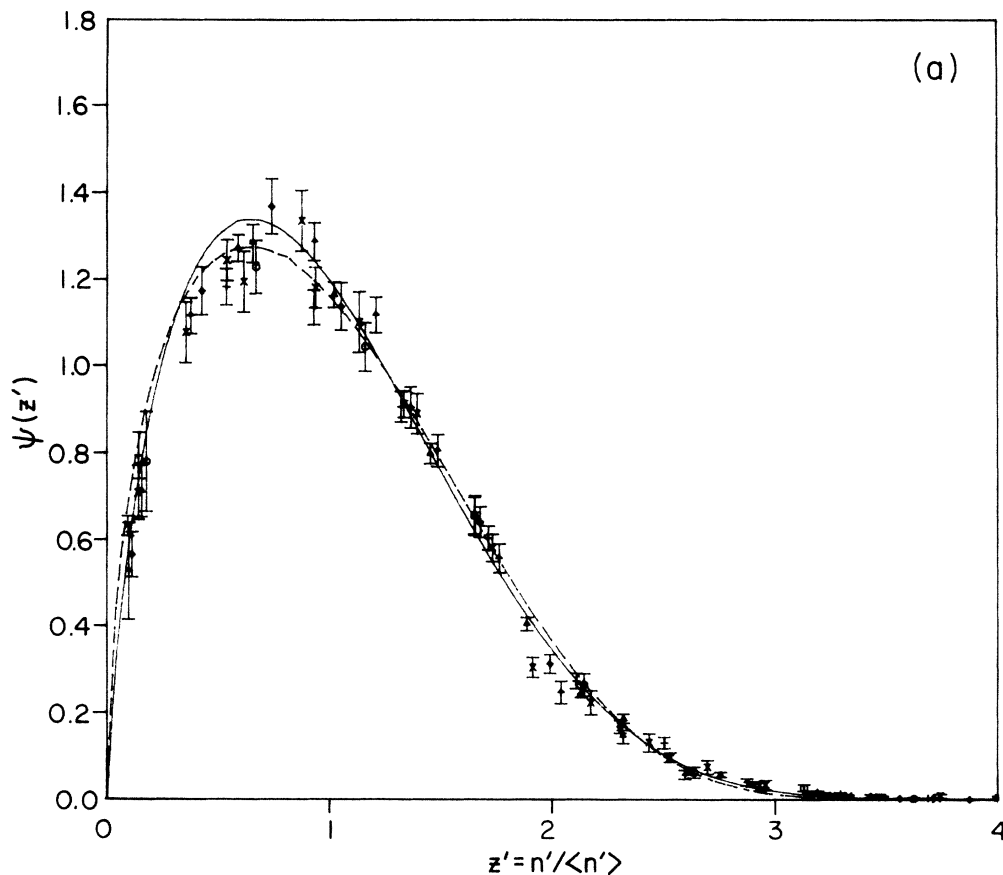


FIG. 1. Evidence for inclusive KNO scaling in z' through the Serpukhov and Fermilab energy ranges. Data from the fixed-target experiments listed in Ref. 19 cover the laboratory momentum range from 50 to 405 GeV/c. The two theoretical curves correspond to expectations from quark distribution functions taken from the naive quark-parton model (solid line) which we use throughout this article or Eichten, Hinchliffe, Lane, and Quigg²⁰ (dashed line). They represent the uncertainty of our parameter-free prediction, shown on a linear scale in (a) and on a semilogarithmic scale in (b).

tion functions. The physical picture we favor is quite different, with the diquarks remaining after the basic constituent collision, simply producing forward jets, the effects of which are removed by leading particle subtraction.

Another simply calculable quantity is the dispersion $D_2 = (\langle n^2 \rangle - \langle n \rangle^2)^{1/2}$. To proceed, first write

$$(D'_2)^2 \equiv \langle n'^2 \rangle - \langle n' \rangle^2 = (ks^\alpha)^2 (\langle x^{2\alpha} \rangle - \langle x^\alpha \rangle^2), \quad (2.29)$$

whence

$$\frac{D'_2}{\langle n' \rangle} = \left[\frac{\langle x^{2\alpha} \rangle - \langle x^\alpha \rangle^2}{\langle x^\alpha \rangle^2} \right]^{1/2} = C, \quad (2.30)$$

where again, in terms of the Pochhammer symbols [Eq. (2.26)],

$$\langle x^{2\alpha} \rangle = \left(\frac{1}{2}\right)_{2\alpha} / \left(\frac{9}{2}\right)_{2\alpha}, \quad (2.31)$$

$$\langle x^\alpha \rangle = \left(\frac{1}{2}\right)_\alpha / \left(\frac{9}{2}\right)_\alpha. \quad (2.32)$$

To obtain D_2 , we replace $n' = n - n_0$,

$$\frac{D'_2}{\langle n' \rangle} = C = \left[\frac{\langle (n - n_0)^2 \rangle - \langle n - n_0 \rangle^2}{\langle n - n_0 \rangle^2} \right]^{1/2} = \left[\frac{\langle n^2 \rangle - \langle n \rangle^2}{\langle n \rangle^2 - 2n_0 \langle n \rangle + n_0^2} \right]^{1/2} \quad (2.33)$$

so that

$$D_2 = C \langle n \rangle \left[1 - \frac{2n_0}{\langle n \rangle} + \frac{n_0^2}{\langle n \rangle^2} \right]^{1/2} = C(\langle n \rangle - n_0), \quad (2.34)$$

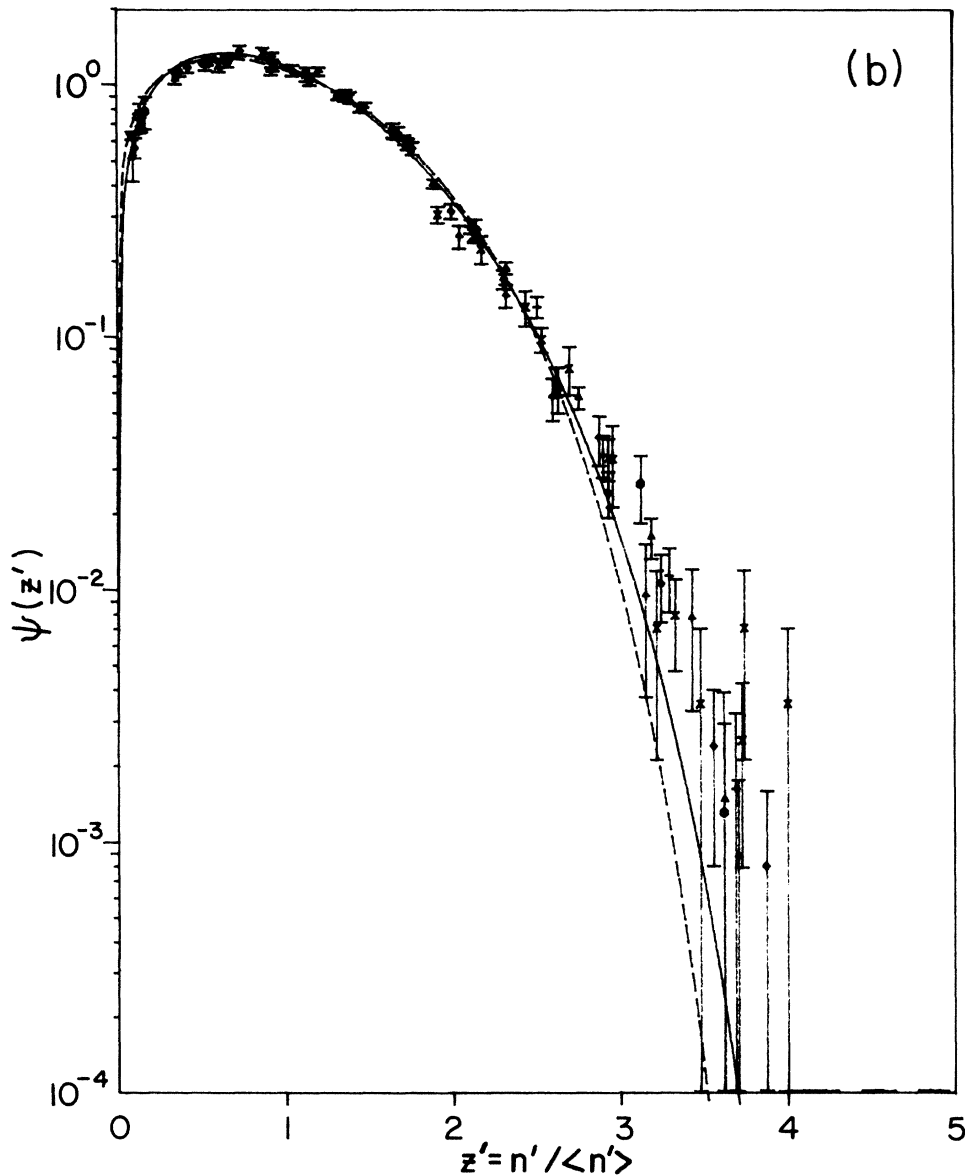


FIG. 1. (Continued).

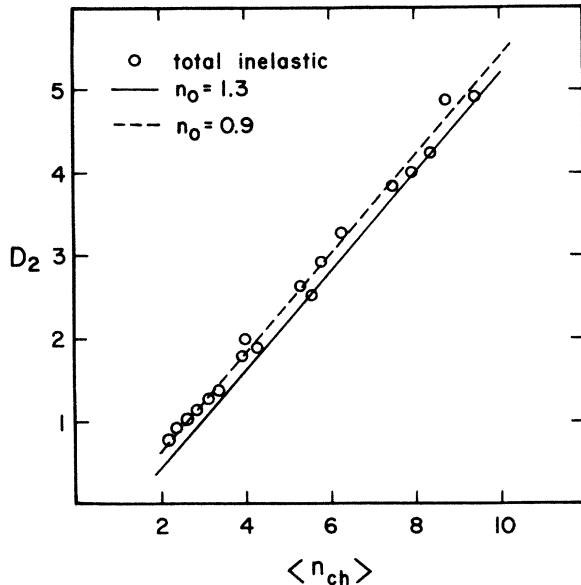


FIG. 2. Data for the dispersion D_2 as a function of the average charged multiplicity as obtained from Ref. 10 compared to the derived Wroblewski relation [Eq. (2.35)] for various values of n_0 .

which is in fact the Wroblewski relation.¹⁴ The constant C appearing in Eq. (2.34) is precisely calculable from Eqs. (2.30)–(2.32), so that $\langle x^{1/2} \rangle = \frac{35}{128}$ and $\langle x^{1/4} \rangle = \frac{16}{33}$, which gives $C = 0.594$. The final formula is thus

$$D_2 = 0.594(\langle n \rangle - n_0) = 0.594\langle n' \rangle \quad (2.35)$$

as postulated by Wroblewski. This formula is compared in Fig. 2 with total inelastic data up to Fermilab/SPS energies (from a compilation in Ref. 10), for $n_0 = 1.3$ (solid line) and $n_0 = 0.9$ (dashed line) which is the most up to date best fit value (see Ref. 11). The latter value gives a perhaps slightly better fit to the low-energy points, but in both cases, agreement with the data is quite good, as seen in Fig. 2. The low-energy points have such a low value of $\langle n' \rangle$ (less than 3) that our model may not really be applicable there. Consequently, in the rest of the paper, we shall stick with the value $n_0 = 1.3$.

We now turn to an extension of this picture to the region of rising cross sections, ascribed to the onset of effects due to gluon-gluon collisions. The presence of two components in the inelastic cross section in fact leads to a modification of the simple power-law behavior of the charged-particle multiplicity [Eq. (2.8)] as well as to an inevitable violation of KNO scaling with increasing c.m. energy.

III. GLUONS AT THE ORIGIN OF KNO-SCALING VIOLATION

As we have mentioned in the Introduction, many authors⁸ have ascribed the rise of the total cross sections after Fermilab energies to the increased activity of gluons inside hadrons. Since the parton model requires the

gluons to have a different distribution than quarks, it is natural, in our picture, to expect that the scaling curve typical of quarks at low energies, as described in the preceding section, will evolve slowly into a different scaling curve typical of gluons at asymmetric energies. We shall, in this section, quantify the manner by which this change occurs.

Faced with a variety of possible parametrizations²³ of the inelastic cross section (or the total cross section if σ_{el}/σ_{tot} remains constant), we choose the simplest possible one

$$\begin{aligned} \sigma_{inel}(s) &= 32.6 + 0.32 \ln^2 \left[\frac{s}{s_0} \right] \\ &= \sigma_0 + \sigma_1 \ln^2 \left[\frac{s}{s_0} \right] \end{aligned} \quad (3.1)$$

with $s_0 = 243.6 \text{ GeV}^2$. This is of the same form (and with the same s_0) as the total cross-section parametrizations of Bourrely and Martin²⁴

$$\sigma_{tot}(s) = 39.23 + 0.43 \ln^2 \left[\frac{s}{s_0} \right] \quad (3.2)$$

consistent with a qualitative saturation of the Froissart-Martin²⁵ bound. Together, these equations imply a slow rise of σ_{el}/σ_{tot} as we reported by the UA4 and UA1 Collaborations.²⁶ Below s_0 we identify these parametrizations as representing the quark component $\sigma_q(s)$ only, thus recovering the scaling demonstrated in Sec. II. Above s_0 , these equations are interpreted as

$$\sigma(s) = \sigma_q + \sigma_g(s) \quad (3.3)$$

with σ_q being the energy-independent first term of Eqs. (3.1) and (3.2).

Conventional naive-parton-model wisdom would require that $f_g(x) \propto (1-x)^5/x$ at Q^2 of a few GeV^2 , which would violate our requirement that $q < 1 - \alpha$ for a well-defined small z' behavior. However the low- x , low- Q^2 behavior of $f_g(x)$ is not known. Theoretically this remains the central problem of soft QCD. Experimentally,²⁰ no data exists below $x = 0.01$ and only sparse data between $0.01 \leq x \leq 0.1$. We feel, therefore, at liberty to cut off $f_g(x)$ in this allowed region at $0.01 \leq x_C \leq 0.1$. Furthermore, for simplicity, we will restrict the small- x behavior to follow that of $f_q(x)$, as was proposed by Eichten, Hinchliff, Lane, and Quigg.²⁰ Requiring continuity at x_C , we thus have a one-parameter phenomenological gluon distribution

$$f_g(x) = \begin{cases} f_g'(x) = 3(1-x)^5/x, & \text{for } x \geq x_C, \\ \left[\frac{x_C}{x} \right]^{1/2} f_g'(x_C), & \text{for } x \leq x_C \end{cases} \quad (3.4)$$

For our applications, such a simple parametrization will suffice. Only more measurements at different collider energies would help us pin down more effectively the form of $f_g(x)$.

A two-component model for multiplicity distributions

will yield a two-component expression for the observed average charged multiplicity $\langle n \rangle$. It is easy to see what form this expression must have if we assume that, event by event, the collision is either of qq or gg origin. We then have to incoherently superpose two multiplicity distributions $F_i(n')$, $i = q$ or g , to form the total multiplicity distribution

$$F(n') = F_q(n') + F_g(n'). \tag{3.5}$$

Each of these topological cross-section distributions is normalized to the appropriate cross section

$$\sum_{n'} F_i(n') = \sigma_i \tag{3.6}$$

and has its own average multiplicity

$$\sum_{n'} n' F_i(n') = \bar{n}'_i \sigma_i \tag{3.7}$$

with

$$\bar{n}'_i = k \langle x^\alpha \rangle_i^2 s^\alpha \tag{3.8}$$

$\langle x^\alpha \rangle_q$ as before and $\langle x^\alpha \rangle_g$ now well defined by the cut-off procedure (3.4) and smaller than $\langle x^\alpha \rangle_q$ because of the predominance of glue at smaller x . Hence, we define the "relative inelasticity" parameter:

$$\eta = \left[\frac{\langle x^\alpha \rangle_g}{\langle x^\alpha \rangle_q} \right]^2 < 1. \tag{3.9}$$

Taking the average of (3.5) we have

$$\begin{aligned} \langle n' \rangle &\equiv \frac{\sum_{n'} n' F(n')}{\sum_{n'} F(n')} = \frac{1}{\sigma_{\text{inel}}} \sum_i \sum_{n'} n' F_i(n') \\ &= \frac{1}{\sigma_{\text{inel}}} \sum_i \bar{n}'_i \sigma_i, \end{aligned} \tag{3.10}$$

where we have used the fact that

$$\sum_{n'} F(n') = \sum_i \sum_{n'} F_i(n') = \sigma_q + \sigma_g = \sigma_{\text{inel}}$$

by (3.3). This can be rewritten as the weighted sum

$$\langle n' \rangle = \bar{n}'_q P_q + \bar{n}'_g P_g \tag{3.11}$$

with the energy-dependent probabilities

$$P_q(s) = \frac{\sigma_q(s)}{\sigma_{\text{inel}}(s)}, \quad P_g(s) = \frac{\sigma_g(s)}{\sigma_{\text{inel}}(s)} \tag{3.12}$$

of the event being initiated by quark or glue collisions, respectively. Inserting (3.8) and (3.9) into (3.11), we finally get

$$\langle n' \rangle = B s^\alpha \frac{\sigma_q(s) + \eta \sigma_g(s)}{\sigma_{\text{inel}}(s)} \tag{3.13}$$

with $B = k \langle x^\alpha \rangle_q^2$.

The formalism to construct $\psi(z')$ from $\langle n' \rangle \sigma_n / \sigma_{\text{inel}}$ is the same as before. Each contribution is given by equations of the same form as (2.14) with an appropriate mean

\bar{n}'_i (instead of $\langle n' \rangle$) and an appropriate K_i [as in Eq. (2.15)] for each process $i = q$ or g

$$\bar{n}'_i \sigma_{ni} = \frac{\sigma_i}{K_i} \frac{\mathcal{G}_i(\rho_i)}{I_i^{(1)}} \tag{3.14}$$

with

$$\mathcal{G}_i(\rho_i) = \rho_i^{1/\alpha-1} \int_{\rho_i^{1/\alpha}}^1 f_i(x) f_i(\rho_i^{1/\alpha}/x) \frac{dx}{x}. \tag{3.15}$$

The i th scaling variable is just

$$0 \leq \rho_i = \frac{n'}{\bar{n}'_i K_i} = \frac{z'_i}{K_i} \leq 1 \tag{3.16}$$

and the requirement that each process gives mean multiplicity \bar{n}'_i is equivalent to requiring that

$$\frac{I_i^{(2)}}{I_i^{(1)}} K_i = 1, \tag{3.17}$$

where the maximum allowed values for z'_i are given by K_i

$$K_q = \frac{1}{\langle x^\alpha \rangle_q^2}, \quad K_g = \frac{1}{\langle x^\alpha \rangle_g^2} = \frac{K_q}{\eta} > K_q \tag{3.18}$$

and the normalization integrals $I_i^{(n)}$ are just

$$\begin{aligned} I_i^{(1)} &= \int_0^1 \mathcal{G}_i(\rho_i) d\rho_i, \\ I_i^{(2)} &= \int_0^1 \mathcal{G}_i(\rho_i) \rho_i d\rho_i. \end{aligned} \tag{3.19}$$

The total $\psi(z')$ subject to the normalization conditions (2.17) is then

$$\psi(z') = 2 \sum_i \frac{\sigma_i}{\sigma_{\text{inel}}} \frac{\langle n' \rangle}{\bar{n}'_i} \frac{I_i^{(2)}}{I_i^{(1)2}} \mathcal{G}_i(\rho_i). \tag{3.20}$$

Note that the maximal value of $z' = n' / \langle n' \rangle$ occurs for $x_1 = 1 = x_2$ and has a common value $K(s)$ for both processes

$$K(s) = \frac{K_q \sigma_{\text{inel}}}{\sigma_q + \eta \sigma_g} = \frac{K_g \sigma_{\text{inel}}}{\sigma_q / \eta + \sigma_g} \tag{3.21}$$

by (3.13) and (3.18). Clearly as $s \rightarrow 0$, $\sigma_{\text{inel}} \rightarrow \sigma_q$ and $K(s) \rightarrow K_q$, while as $s \rightarrow \infty$, $\sigma_{\text{inel}} \rightarrow \sigma_g$, and $K(s) \rightarrow K_g > K_q$. The signal for the onset of gluon-initiated processes is thus the appearance of large z' events despite the fact that $\langle x^\alpha \rangle_g < \langle x^\alpha \rangle_q$. One should however remark that the functions $\mathcal{G}_i(\rho_i)$ become too small to be measurable experimentally well before $\rho = z' / K \rightarrow 1$ or equivalently

$$\rho_i = \rho \frac{K}{K_i} \frac{\langle n' \rangle}{\bar{n}'_i} \rightarrow 1$$

for each $i = q, g$. This explains why the experimentally observable $\psi(z')$ does not extend all the way up to $K(s)$. Indeed, if $f_i(x) \propto (1-x)^{n_i}$ at large x , one can show that this implies

$$\psi_i(z') \propto (1-\rho_i^2)^{2n_i} \text{ as } \rho_i \rightarrow 1 \tag{3.22}$$

which becomes negligible at smaller ρ_i as n_i increases. Hence the glue contribution will remain less important

than the quark one at large z' even at relatively high energies.

We shall fix the parameters of our model α , x_C , and B in the most straightforward way.

(1) From Sec. II we know that $\alpha = \frac{1}{4}$ provides a good low-energy KNO-scaling curve. Only small variations are allowed ($\alpha = 2.45$) and these are discussed in Sec. V. Note that the low- and high-energy limits of (3.13) are

$$\langle n' \rangle = \begin{cases} Bs^\alpha, & \text{for } s < s_0, \\ B\eta s^\alpha, & \text{as } s \rightarrow \infty. \end{cases} \quad (3.23)$$

The standard extrapolation of Bs^α which was considerably too large at high energies is thus naturally reduced by a factor $\eta < 1$. Various fits of the type in (3.13) are discussed elsewhere.¹⁵

(2) The value of x_C (and thus of η) is determined by the KNO inclusive curve at the $Spp\bar{p}S$ since the collider is the only machine where the glue has become (relatively) important.

(3) The value of B is fitted to data on $\langle n \rangle = \langle n' \rangle + 1.3$ at all energies.

We find that $\alpha = \frac{1}{4}$, $x_C = 0.03$ (thus $\eta = 0.658$) and $B = 1.40$ provide a good fit to $\langle n \rangle$ and $\psi(z')$ data at all energies. In Fig. 3, we show $\psi(z')$ data through the ISR

energy range on both linear [Fig. 3(a)] and semilogarithmic [Fig. 3(b)] graphs, together with the "scaling" curve at a typical energy (taken to be $\sqrt{s} = 52.8$ GeV) and its decomposition into the main quark component and the small glue contribution. Because this increasing glue contribution is still quite small at the ISR, the data "scales" within the experimental errors. Figures 4(a) and 4(b) display the situation at the $Spp\bar{p}S$ energy of $\sqrt{s} = 540$ GeV, which, being the highest energy attained up to now, has the largest glue contribution and a more significant scaling violation than at the ISR. Just as we could analytically perform the integration leading to $\psi_q(z')$ of Eq. (2.24), we have been able to obtain a similar (but much more lengthy) expression for $\psi_g(z')$.

The main point that we want to stress here is that the same mechanism which lowers the multiplicities $\langle n \rangle$ expected in a pure Bs^α parametrization leading to KNO scaling must have $\eta < 1$ (as glue does) and thus generates scaling violation by increasing the values that $n'/\langle n' \rangle$ can attain. The mechanism by which our model generates extra events at large z' is thus quite straightforward but unconventional. Adding a gluon contribution with $\bar{n}'_g < \bar{n}'_q$ lowers the expected $\langle n' \rangle$ and this leads to $z' = n'/\langle n' \rangle$ reaching larger values. Normalizing $\psi(z')$ does not remove these large z' events but does alter the

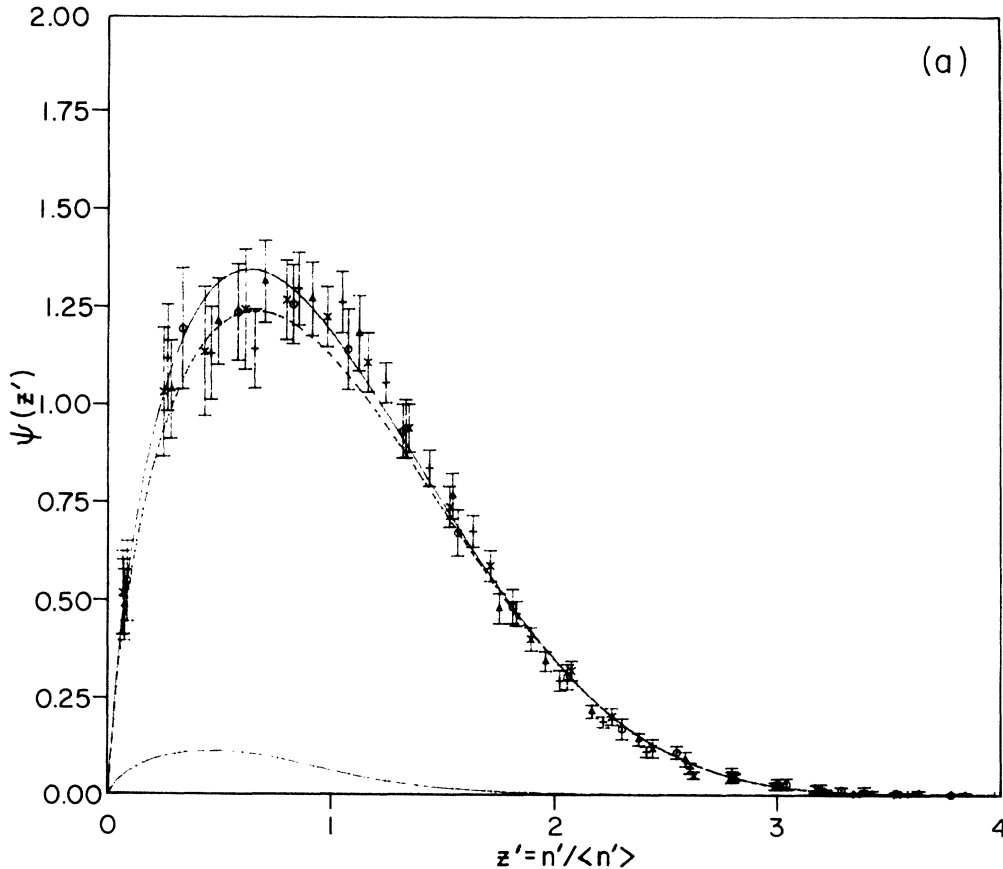


FIG. 3. Evidence for inclusive KNO "scaling" in z' through the ISR energy range using the data of Breakstone *et al.* (Ref. 27). The solid curve represents the prediction at $\sqrt{s} = 52.6$ GeV and it is decomposed into the energy-independent quark component (short-dashed line) and the much smaller energy-dependent (scale-violating) glue component (long-dashed line). We again show the good overall agreement on the linear graph (a) and the good large z' agreement on the semilogarithmic graph (b).

overall shape of the curve for all z' .

The resulting $\langle n \rangle$ fit is quite satisfactory as can be seen in Fig. 5 where the energy range extends up to the Tevatron Collider. The dashed curves are meant to indicate "error bars" for our prediction, corresponding to $x_C = 0.03 \pm 0.01$ best fits to $\langle n \rangle$ with $\alpha = \frac{1}{4}$ still. At the SppS energy of $\sqrt{s} = 900$ GeV, for example, we predict $\langle n \rangle = 37-38$. Lowering α to 0.245 can result in lowering $\langle n \rangle$ at that energy by about 1 unit. At $\sqrt{s} = 2$ TeV, we predict similarly $\langle n \rangle = 54-57$ and $51-54$, respectively, assuming $\sigma_{\text{tot}}(s)$ to continue to qualitatively saturate the Froissart bound. Any slower increase of $\sigma_{\text{tot}}(s)$ would increase our estimate of $\langle n \rangle$ at higher energies.

Another important but more technical point should be

made at this time. Because of Eqs. (3.17) taken together with the definitions in (3.19), the maximal z'_i values K_i are independent of the normalizations of the distribution functions $f_i(x)$. This entails that $K(s)$ is also independent of the normalizations of the $f_i(x)$ and that the same holds true for $\bar{n}'_i \sigma_{ni}$ of (3.14) or $\psi(z')$ of (3.20). This dependence upon the shape of the $f_i(x)$ [or the $\mathcal{G}_i(\rho_i)$] and not their normalization, is due to our requirement that the strength of each contribution be normalized to its contribution to the experimental σ_{inel} and that furthermore its first moment give \bar{n}'_i which is also an experimentally fitted quantity, given that (3.11) or (3.13) must reproduce the data.

We have also checked that normalizing the quark and

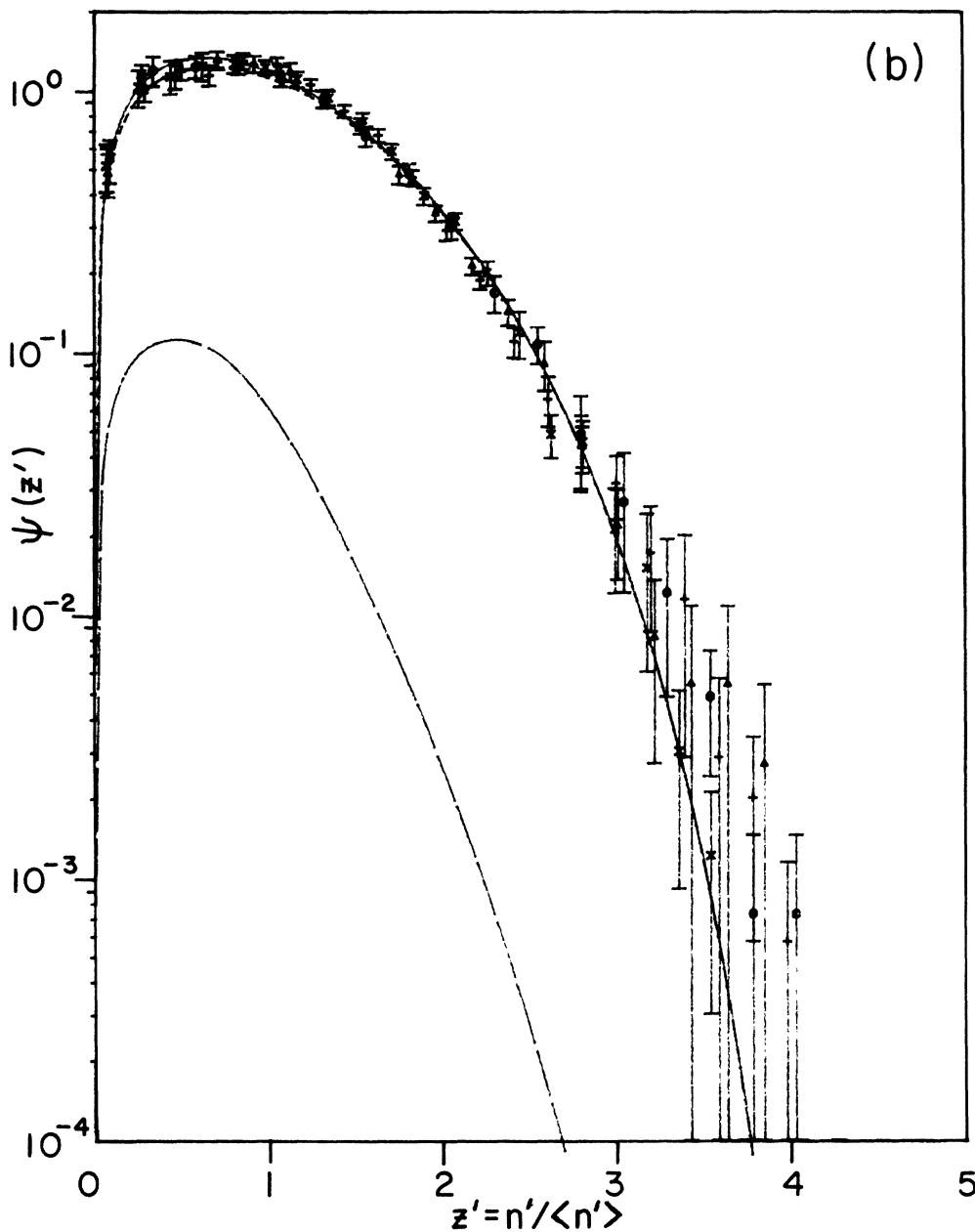


FIG. 3. (Continued).

glue contributions in $\psi(z')$ as they appear in (3.20) via the ratios $\sigma_i/\sigma_{\text{inel}}$ to the ratios $\sigma_i/\sigma_{\text{tot}}$ instead, does not affect our results and leads to an imperceptible difference in any of the preceding figures. We can thus, in a first approximation, ignore the clear increase in $\sigma_{\text{el}}/\sigma_{\text{tot}}$ seen by UA (Ref. 26). It is instead the increase of $\sigma_{\text{tot}}(s)$, which we ascribe to gluons, which is responsible for KNO-scaling violation. The increase in $\sigma_{\text{el}}/\sigma_{\text{tot}}$ may have the same origin, but we would consider it a consequence rather than a cause of KNO-scaling violation.

A side-by-side comparison of Figs. 3 and 4 reveals that the inclusive data does not strongly violate KNO scaling. This mild violation can be restated in terms of the moments C_j'

$$C_j' = \langle z'^j \rangle = \frac{\langle n'^j \rangle}{\langle n' \rangle^j} \quad (3.24)$$

which are seen in Fig. 6 to slowly vary with energy. Note that, at low energies, our prediction is parameter free (given $\alpha = \frac{1}{4}$) and that, at all other energies, it depends only on one parameter x_C (or η), given that B is determined from data once η is known. The coefficients C_j' were obtained exclusively from experiments where the σ_n are tabulated;²⁹ they are in general larger than the usual

$C_j = \langle n^j \rangle / \langle n \rangle^j$ which are themselves larger²⁷ than the corresponding coefficients for the non-single-diffractive (NSD) data. We should stress that it is this NSD data which shows the largest KNO-scaling violation and we turn to understanding this phenomenon in the following section.

IV. THE QUESTION OF NON-SINGLE-DIFFRACTIVE (NSD) DATA

It has long been argued that KNO scaling should apply better to inelastic data with single-diffractive-dissociation events removed, resulting in scaling of the so-called non-single-diffractive (NSD) inelastic data. Breakstone *et al.*²⁷ have found that NSD events satisfied KNO scaling within experimental errors through the ISR energy range, while UA5 (Ref. 30) has found a very significant KNO scale breaking in the NSD data at the $Spp\bar{p}S$ compared to that of the ISR.

In our model such a removal of single-diffractive (SD) events is artificial and we prefer to show the total inclusive data. We can however remove the SD events in a simple way which we now describe. Our conclusions will be that, subject to removal of the experimentally "ob-

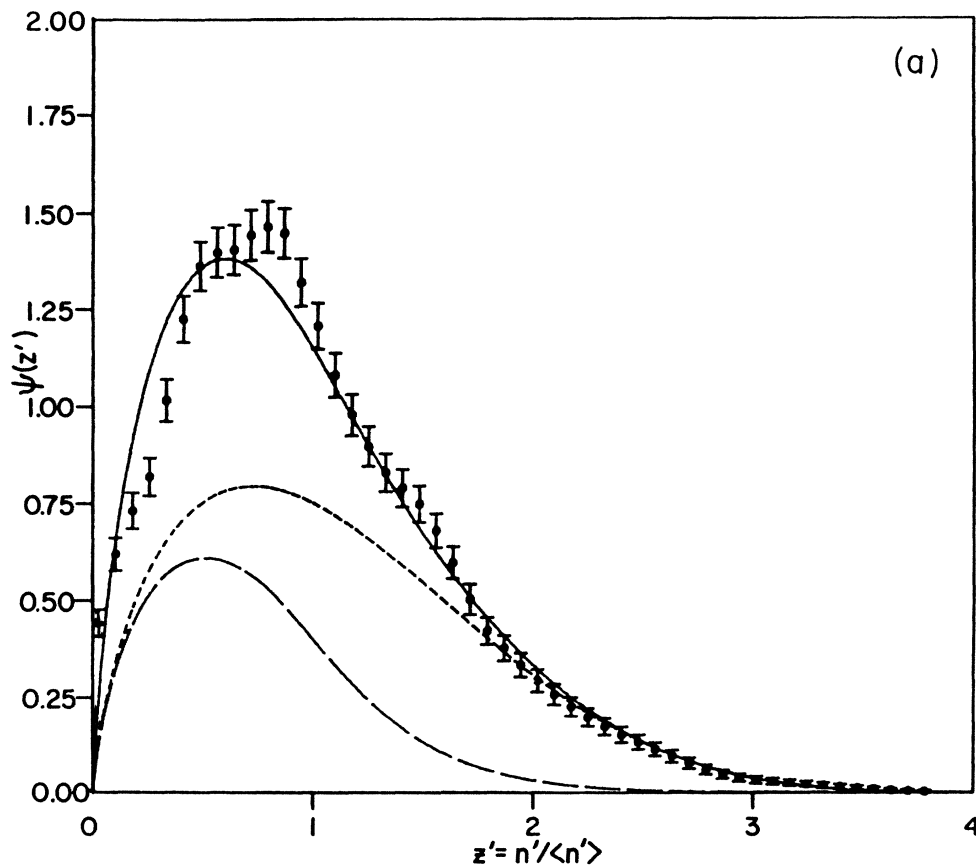


FIG. 4. The same quantities as in Fig. 3 are plotted now at the $Spp\bar{p}S$ energy of $\sqrt{s} = 540$ GeV. The data (from Ref. 11), as well as the theoretical curve, are not compatible with the "scaling" curve displayed in Fig. 3, especially at large z' . For the theoretical curve, the effect is most easily seen by the larger value of z' that can be reached at the higher energy.

served" SD component, the $Spp\bar{S}$ NSD data is seen to naturally break KNO scaling much more than the inclusive data does for the simple reason that $\langle n \rangle$ is multiplicatively less rescaled at the $Spp\bar{S}$ than at the ISR.

Our subtraction method will again be taken to be the simplest possible. We will test it with the ISR data of Breakstone *et al.*²⁷ and then predict the $Spp\bar{S}$ observations. Let us make the following simple experimental observation: an SD event is usually identified by noting the absence in one arm of the detector (say arm 1) of any charged particle (or seeing at most one leading particle with a very large x). This means that the available x_1 for the fireball production must be very small, less than a given experimental cutoff $x_{CE} \ll 1$. There are no restrictions on the observed particles in arm 2 or on the corre-

sponding x_2 value. It therefore seems, short of doing a full Monte Carlo simulation, that enforcing a lower cutoff limit on the integral in (3.15) would cutoff the undesired SD events.

Equations (3.20) and (3.15), respectively, become

$$\tilde{\psi}(z') = 2 \sum_i \frac{\tilde{\sigma}_i}{\tilde{\sigma}_{inel}} \frac{\langle \tilde{n}' \rangle}{\tilde{n}'_i} \frac{\tilde{I}_i^{(2)}}{\tilde{I}_i^{(1)2}} \tilde{\mathcal{G}}_i(\rho_i), \quad (4.1)$$

$$\tilde{\mathcal{G}}_i(\rho_i) = \rho_i^{1/\alpha-1} \int_{\max(\rho_i^{1/\alpha}, x_{CE})}^1 f_i(x) f_i(\rho_i^{1/\alpha}/x) \frac{dx}{x}, \quad (4.2)$$

where the tilde refers to the usual quantities but for the NSD data set only. The normalization integrals $\tilde{I}_i^{(n)}$ are

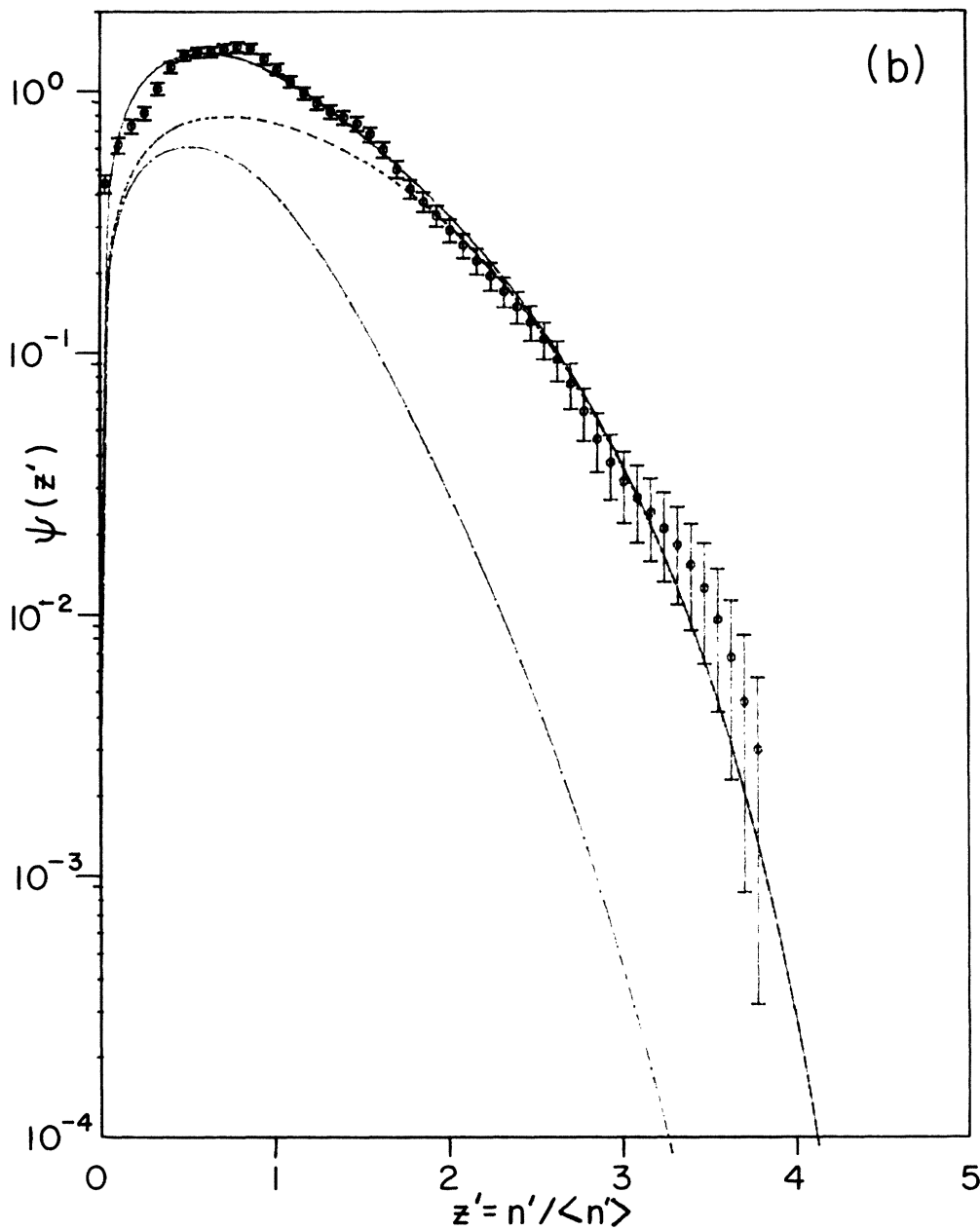


FIG. 4. (Continued).

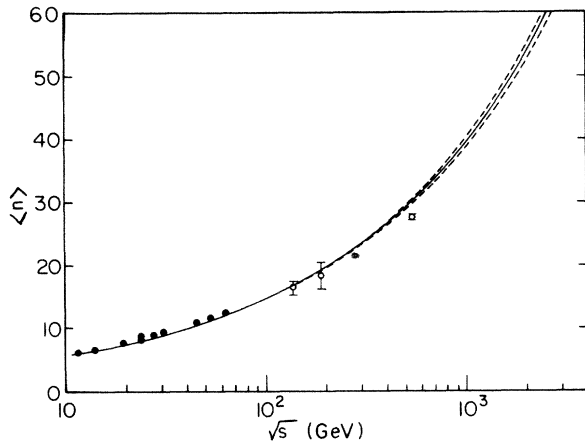


FIG. 5. Fit of the average charged multiplicity $\langle n \rangle = \langle n' \rangle + 1.3$ as a function of energy from $\sqrt{s} = 10$ GeV to the Tevatron energy range, using Eq. (3.13) and the parameter values cited in the text. In addition to the data from all of the references listed in Figs. 1, 3, and 4, we have added the cosmic ray data of Ref. 28.

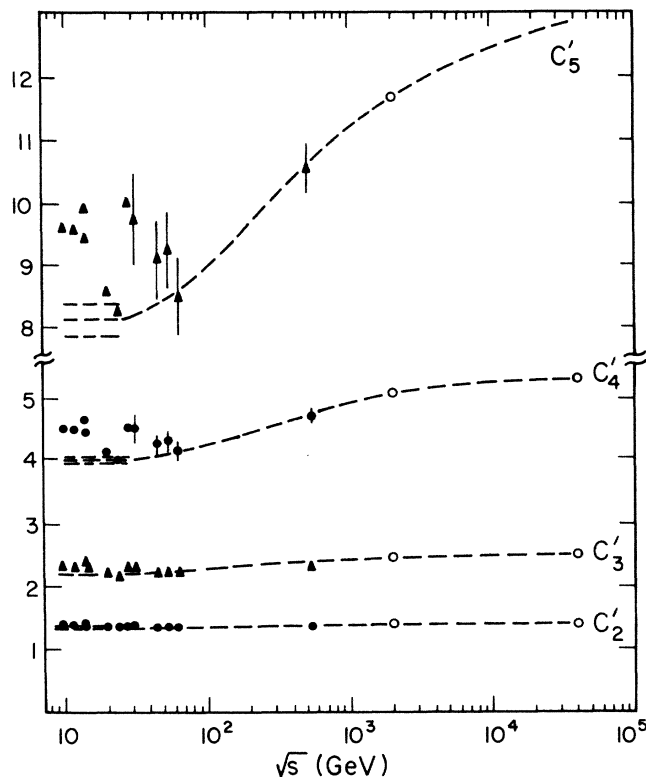


FIG. 6. Data (Refs. 11, 19, and 27) for the first four nontrivial moments $C'_j = \langle z'^j \rangle$ of the inclusive distribution as obtained from the same references as for Figs. 1, 3, and 4 ($C'_1 = 1$ by definition). Error bars (when shown) are evaluated from the corresponding ones for the $C_j = \langle z^j \rangle$ (when these are given by the experiments) by assuming that they are of the same percentage. The experiments where we show no error bars have lower statistics than the ones where we do show errors; hence the statistical errors on these experiments would be even larger. At lower energies, where scaling holds, the magnitude of the theoretical error bands correspond to using the two-quark distribution functions shown in Fig. 1.

obtained by equations similar to (3.19) with integrand $\mathcal{G}_i(\rho_i)$. Note that the integrals (4.2) and (3.15) differ only for $\rho_i > x_{CE}$, i.e., for

$$z' > (K_i \bar{n}' / \langle n' \rangle) x_{CE}^\alpha.$$

Given that the bracket has value $\simeq 4$ and that, at the ISR, only $z' \lesssim 1$ events are affected by the SD subtraction, one roughly expects that $x_{CE} \simeq (\frac{1}{4})^{1/\alpha} \simeq 0.004$ which is a very small number indeed. This same value must reproduce the full $\tilde{\psi}(z')$ shape for all z' and account for the experimental σ_{SD} which one obtains in our model by comparing $I_i^{(1)}$ and $\tilde{I}_i^{(1)}$ and summing over the two components.

The result of this exercise at $\sqrt{s} = 52.8$ GeV is shown in Fig. 7 compared to the full ISR data. One has correctly reproduced the small z' subtraction resulting in a σ_{SD} value of 5.5 mb (for $x_{CE} = 0.005$) which is in remarkable agreement with the estimate of 15% SD events found by Breakstone *et al.*²⁷ but slightly smaller than the values of Conta *et al.*³¹ We have also obtained an $\langle \bar{n}' \rangle$ which is larger than $\langle n' \rangle$ by 1.2 units (since $\tilde{I}_i^{(2)} > I_i^{(2)}$) in agreement with the experiment. We have thus, through the definition of z' which reads for the NSD data $z' = n' / \langle \bar{n}' \rangle$, obtained an NSD curve which ends earlier in z' than the inclusive one, i.e., is narrower; because of the normalization condition (2.17) it is also higher at the maximum, as observed experimentally. It should also be clear that the extent of narrowing is proportional to how different $\langle \bar{n}' \rangle / \langle n' \rangle$ is from 1, since this ratio enters in the ratio of the abscissas of the graphs of $\tilde{\psi}(z')$ and $\psi(z')$. The larger this ratio, the larger the difference between the “scaling” curves at any given energy. Since at the $Spp\bar{p}S$ this ratio is much closer to 1 than at the ISR, the $Spp\bar{p}S$ curves $\tilde{\psi}(z')$ and $\psi(z')$ are much more similar to each other than those at the ISR are between themselves. Comparing a $\tilde{\psi}_{Spp\bar{p}S}(z')$ which is nearly as wide as $\psi_{Spp\bar{p}S}(z')$ with a much narrower $\tilde{\psi}_{ISR}(z')$ naturally results in claiming a large KNO-scaling violation. The $Spp\bar{p}S$ curve shown in Fig. 8 has a cutoff value of $x_{CE} = 0.001$, corresponding to $\sigma_{SD} = 3.8$ mb and $\langle \bar{n}' \rangle - \langle n' \rangle = 1.9$ which are within the experimental errors for these quantities.

Because the glue contribution is concentrated at smaller z' than the main quark contribution, such as is displayed in Fig. 3 at the ISR, the cutoff procedure with x_{CE} removes a large fraction of it, resulting in a better agreement with KNO scaling, as Breakstone *et al.*²⁷ have found.

Finally, since the determination of x_{CE} depends crucially on the value of σ_{SD} , one has to discuss further the measurements of σ_{SD} as a function of energy. It was found that, at the ISR, single- and double-diffractive dissociation nearly saturated the Pumplin bound³²

$$\sigma_{\text{diff}}(s) \leq \frac{\sigma_{\text{tot}}(s)}{2} - \sigma_{\text{el}}(s) \quad (4.3)$$

and could even account for the totality of the rise in $\sigma_{\text{tot}}(s)$ (Ref. 31). However the recent value of $\sigma_{SD} = 5 \pm 1.5$ mb found by UA5 (Ref. 11) at the $Spp\bar{p}S$ is actually lower than the measurements at the ISR. This casts a serious doubt on our ability to estimate $\sigma_{SD}(s)$ theoretically in a

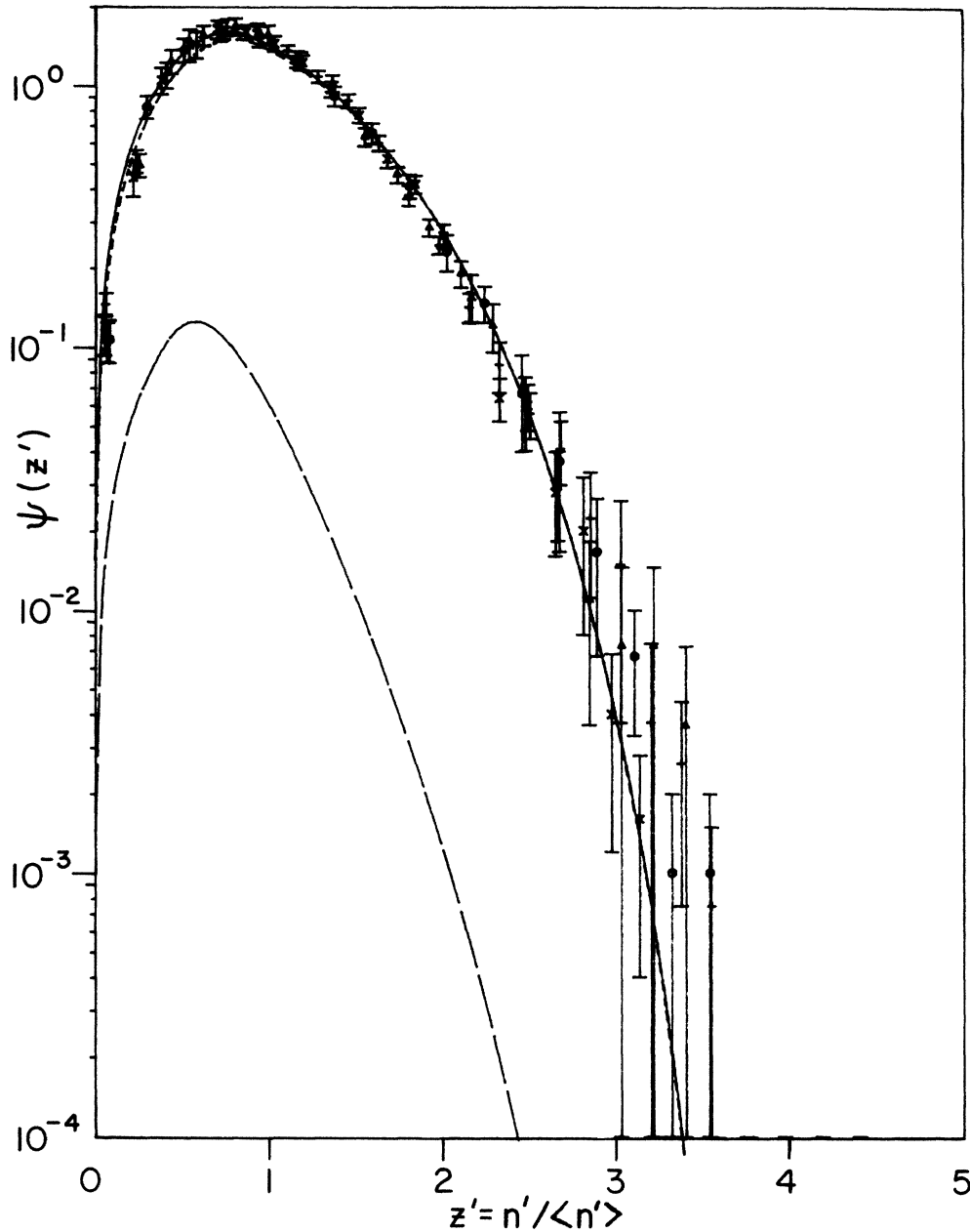


FIG. 7. Evidence for KNO "scaling" in z' of the NSD data through the ISR energy range (Ref. 27). The theoretical curve is decomposed as for Fig. 3. Again the smallness of the glue contribution, which violates scaling through its energy dependence, insures approximate scaling, which is even better than in Fig. 3 since removal of the SD events removes small z' events where the glue is relatively more important. Comparison with Fig. 3 also reveals that both the data and the theoretical curve (which are in excellent agreement) are narrower after subtracting the (small- z') SD events, as well as having a higher maximum, because of the identical normalization conditions.

reliable fashion. In the next section, we therefore concentrate only on predictions for the inclusive $\psi(z')$ at Super Collider energies.

V. PREDICTIONS FOR THE SUPER COLLIDERS

The predictions at higher energies depend significantly on our high-energy parametrization for $\sigma_{\text{tot}}(s)$. Choosing, as we have done, the fastest qualitative energy dependence

compatible with the Froissart bound, tends to maximize the energy dependence of all observables. This is only theoretical prejudice on our part, since parametrizations which asymptotically yield a constant σ_{tot} are also allowed by simultaneous fits of the forward elastic phase

$$\rho(s, t=0) = \text{Re}f_{\text{el}}(s, t=0) / \text{Im}f_{\text{el}}(s, t=0)$$

and the total cross section $\sigma_{\text{tot}}(s) \propto \text{Im}f_{\text{el}}(s, t=0)$ using

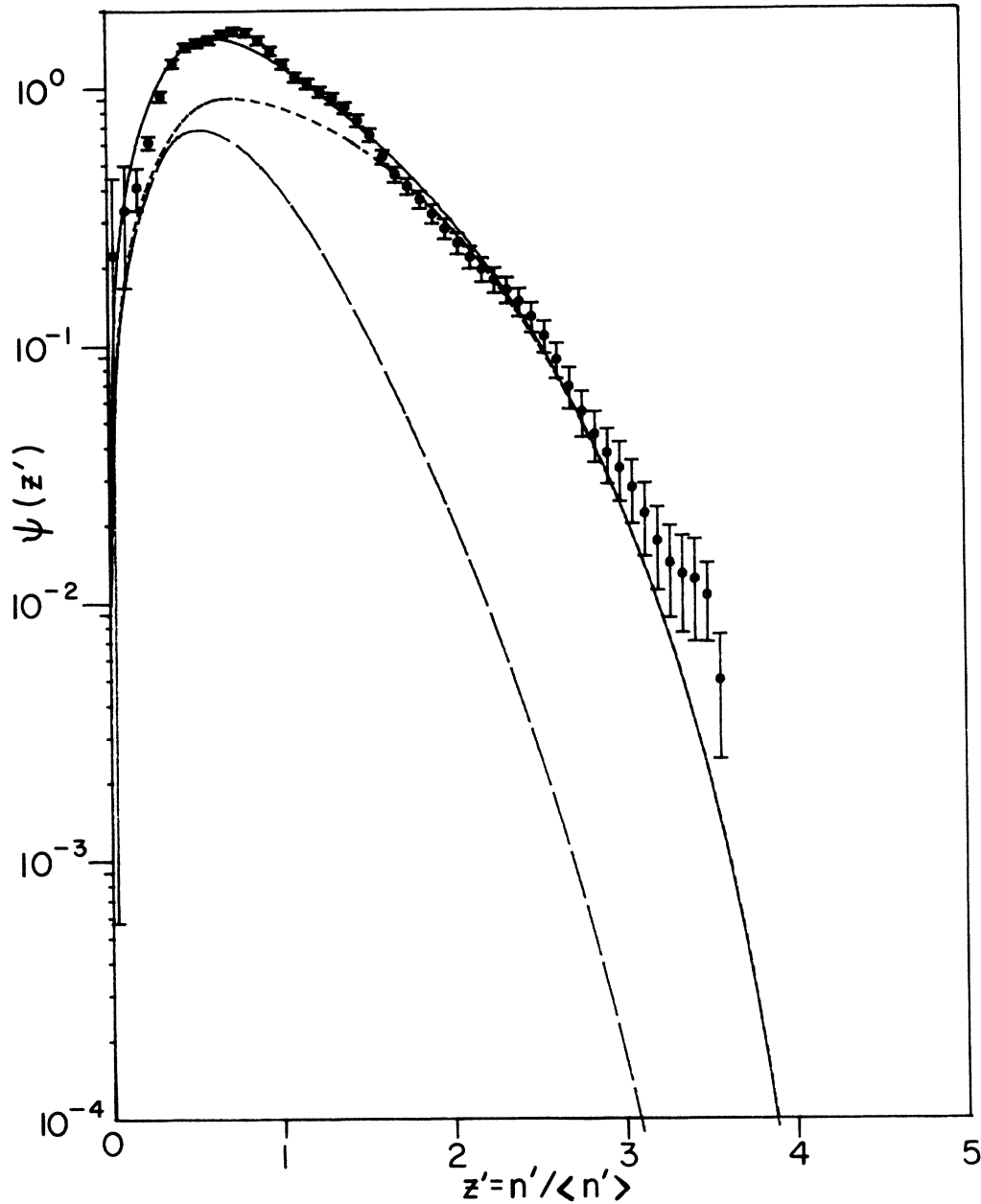


FIG. 8. The same quantities as in Fig. 7 are plotted at the $S\bar{p}\bar{p}S$ energy of $\sqrt{s} = 540$ GeV (Ref. 30). By comparing with Fig. 7, we note that removal of the appropriate number of SD events at each energy has increased the scaling violation. At large z' this translates into the theoretical curve reaching much higher values at the higher energy.

dispersion relations.²⁴ Such a slower rising $\sigma_{\text{tot}}(s)$ would result in a scaling violation which is not as strong as the one we display in Fig. 9 for an $\sigma_{\text{inel}}(s)$ obeying Eq. (3.1). These curves are the ones we predict at the Tevatron energy of $\sqrt{s} = 2$ TeV and the SSC energy of $\sqrt{s} = 40$ TeV and they are shown with their decompositions into quark and glue components. Note that the glue becomes important over a larger region of z' as $s \rightarrow \infty$ but that the quark contribution still dominates at large z' , as Eq. (3.22) dictates. The complete evolution of the scale breaking in $\psi(z')$ is shown in Fig. 10 for 5 c.m. energies $\sqrt{s} = 53$ and 540 GeV, 2 and 40 TeV and “infinite” energy.

These high-energy predictions could also be affected by

our interpretation of the only true parameter of our model η (B and α being given by $\langle n \rangle$ and lower-energy data). We have taken it, up to now, to be a constant, a measure of our present inability to measure $f_g(x)$ at very small x . The cutoff value x_C , which is in a one-to-one correspondence with η (given a fixed α), could also be interpreted as a manifestation of an energy threshold which has this particular value $x_C(s) = 0.03$ at the $S\bar{p}\bar{p}S$, the only accelerator whose data constrains $x_C(s)$ at the moment. If indeed an energy threshold is behind the present value of $x_C(s)$ at the $S\bar{p}\bar{p}S$, η becomes an energy-dependent parameter $\eta(s) = \eta(s_1)(s_1/s)^\alpha$, with $s_1 = (540 \text{ GeV})^2$ and $\eta(s_1) = 0.658$. This affects through Eq. (3.13) the fit for

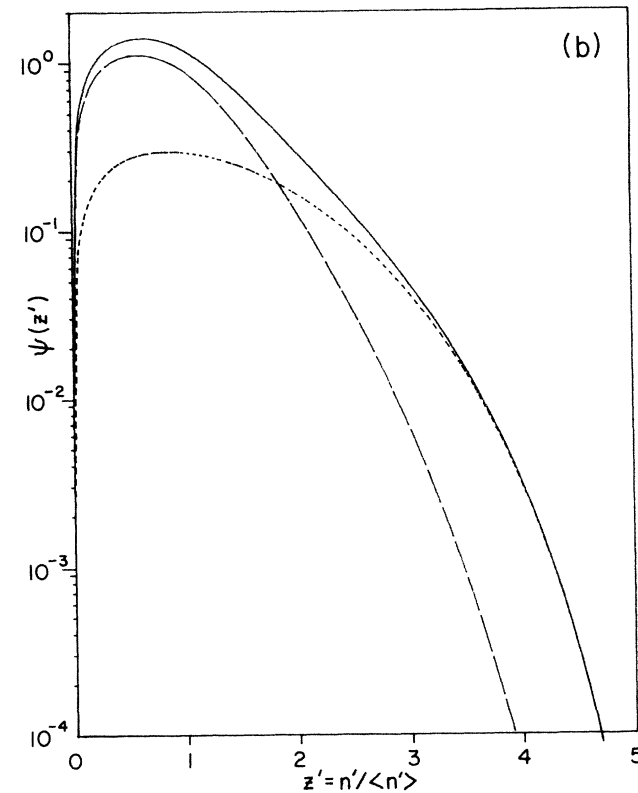
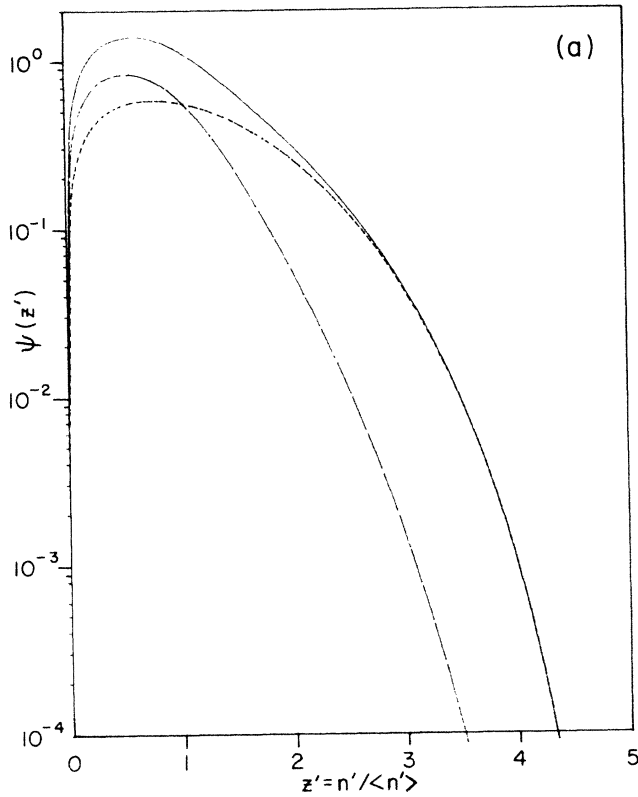


FIG. 9. The solid curves are our predictions for the inclusive KNO function at $\sqrt{s} = 2$ and 40 TeV [(a) and (b), respectively]. The short- and long-dashed curves correspond, respectively, to the quark and glue components, as in Figs. 3 and 4.

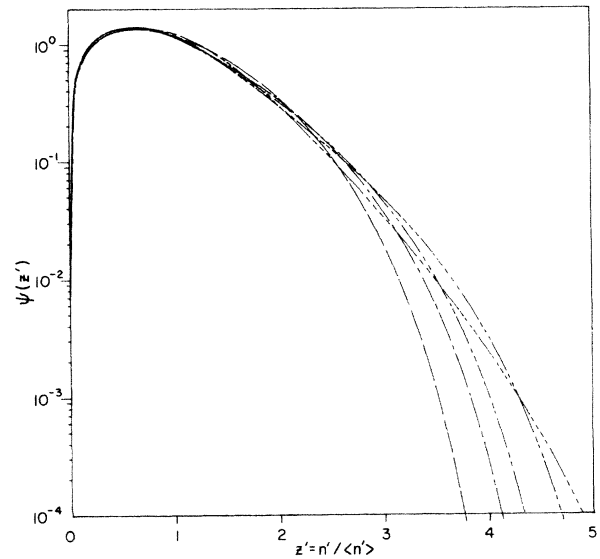


FIG. 10. The evolution of the KNO function as a function of energy. Increasing energy is represented by an increase in the number of short dashes. The energies shown are (in TeV) 0.05, 0.54, 2, 40, and "infinite."

$\langle n \rangle$, which is now displayed in Fig. 11. The asymptotic energy dependence is now much slower and of the form $\langle n \rangle = BP_q s^\alpha \rightarrow Bs^\alpha \sigma_0 / [\sigma_1 \ln^2(s/s_0)]$ as $s \rightarrow \infty$. The resulting energy-dependent cutoff $x_c(s)$ decreases as the energy increases above the $Spp\bar{p}S$, resulting in an asymptotic $\psi(z')$ with a sharp peak at very small z' . Clearly further measurements at higher $Spp\bar{p}S$ energies would help us distinguish between the two possibilities.

Finally, we have discussed in another publication¹⁵ the allowed modification of the power α . Its importance for the KNO-scaling violation is only mildly quantitative.

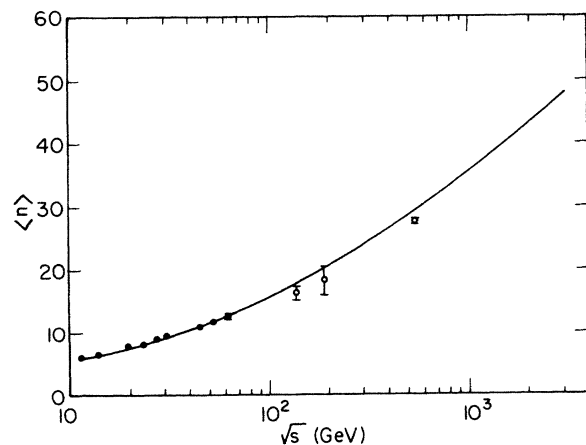


FIG. 11. A fit of the average charge multiplicity as a function of energy in the case of an energy threshold (see text). Note the much lower values reached at higher energies as compared to Fig. 5.

The strength, shape, and origin of the violation are virtually unchanged.

VI. DISCUSSION AND CONCLUSION

The approximate validity of the additive quark model and the simultaneously observed KNO scaling at low energies (below the ISR) strongly suggests that the observed KNO scaling function $\psi(z')$ should be related to the quark distribution function $f_q(x)$. Under the hypothesis of a one-to-one power relation between observed (leading particle removed) multiplicity n' and parton c.m. energy $(\hat{s})^{1/2}$ involved in the collision, i.e., $n' = k\hat{s}^\alpha$ event by event, one can derive an expression relating the two. We have argued that these distribution functions should be evaluated at a low Q^2 and that Q^2 evolution is negligible, a fact confirmed by the s independence of the KNO function below the ISR energy range.

Confronting the data with different distributions $f_q(x)$ we find that our predictions for $\alpha = \frac{1}{4}$ (with their theoretical uncertainties) agree with Serpukhov and Fermilab data within experimental errors. In particular, using the naive-parton-model form, one can obtain a curious parameter-free analytic form which reproduces well the data. We also very simply derive the Wroblewski relation which agrees well with the extensive data at these low energies.

There are several reasons to believe that the increase in hadron-proton total (or inelastic) cross sections is due to the increased activity of the gluons. Making this identification one then expects, at asymptotically large energies, to observe a new KNO function derivable from $f_g(x)$; at any intermediate energy (such as at the $Spp\bar{p}S$) one would observe a transitory scale-violating situation. The overall s -dependent $\psi(z')$ is just obtained from the incoherent sum of qq and gg scaling functions with respective s -dependent weights given by their contribution to $\sigma_{\text{inel}}(s)$ and their means obtained from a two-component fit to the total charged multiplicity $\langle n \rangle(s)$. In order to define \bar{n}'_g one needs to cutoff $f_g(x)$ at a very low value ($x_C = 0.03$), where experiments have very little to say. This constitutes the only parameter of our model, given that the fits to $\sigma_{\text{inel}}(s)$ and $\langle n \rangle(s)$ reproduce the data. At the ISR, when this glue contribution is so small as to be within the experimental errors, the agreement with the data is excellent.

The resulting high-energy values of $\langle n \rangle(s)$ are lower than those expected from simple extrapolation of the low-energy $s^{1/4}$ behavior, by a factor

$$\eta = (\langle x^{1/4} \rangle_g / \langle x^{1/4} \rangle_q)^2$$

at asymptotic energies [cf. Eq. (3.23)], which is less than 1 because the effect of the glue is concentrated at smaller x than for the quarks. The resulting scaling violation predicted by our model compares successfully with the inclusive data. The excess of counts at large z' is due to $\langle n \rangle(s)$ being reduced compared to what one would expect

from a single quark-initiated power behavior which would lead to exact scaling. The energy evolution of the moments $\langle z'^j \rangle$ is also well reproduced.

In view of the much larger scaling violation observed at the $Spp\bar{p}S$ for the NSD data as compared to the inclusive data, we have implemented a simple experimental justifiable cutoff procedure at small z' . This procedure is parameter-free given the experimentally measured SD cross section that we have to subtract. The comparison with the data is also quite good, both at the ISR (where we test the validity of our simplistic subtraction scheme) and at the $Spp\bar{p}S$ where the scaling violation is seen to be stronger than for the inclusive data. We argue that a large part of this effect comes from the small SD cross section and the ensuing small difference between the $\langle n \rangle$'s calculated from both sets of data. At the ISR, the two types of curves are very different because the ratio of these $\langle n \rangle$'s is large; at the $Spp\bar{p}S$, this ratio is smaller and the two types of curves are more similar. A small scale violation in comparing inclusive data can thus be magnified if one compares NSD data between ISR and $Spp\bar{p}S$ energies.

Finally we have presented our model predictions up to c.m. energies of 40 TeV. Because the measurements at the $Spp\bar{p}S$ energy $\sqrt{s} = 540$ constitute our only constraint for our single parameter x_c (or equivalently η), several interpretations for it are possible. We have explored two: the first being, as before, a manifestation of our ignorance of the exact small- x behavior and the second being due to the existence of an energy threshold. Only further anxiously awaited measurements at different collider energies will help us pin down the small- x (small- z') behavior as a function of energy, independent of the very slow (negligible) energy evolution of the distribution functions.

Note added. After this paper had been submitted for publication, we became aware of previous work which explored some consequences of the Eilam-Gell picture of KNO scaling: S. P. K. Tavernier, Nucl. Phys. **B105**, 241 (1976); F. Takagi, Z. Phys. C **13**, 301 (1982); **19**, 213 (1983). We would like to thank F. Takagi for bringing these references to our attention.

ACKNOWLEDGMENTS

We wish to thank T. O. White and the members of the UA5 (Bonn-Brussels-Cambridge-CERN-Stockholm) Collaboration for communicating their data to us (some of it as yet unpublished) in a convenient tabular form. One of us (S.R.) wishes to thank A. Halperin and the Lewes Center for Physics for hospitality while part of this work was done and to acknowledge the research support afforded by the U.S. Department of Energy, under Contract No. DE-AC02-83ER40105 and by the National Science Foundation through the Presidential Young Investigator Program, supplemented by a Grant From the Exxon Education Foundation. The other (P.V.) wishes to thank the Ministère de l'Éducation du Québec for its Chercheur-Boursier program and NSERC for research support.

- ¹UA2 Collaboration, M. Banner *et al.*, Phys. Lett. **118B**, 203 (1983); UA1 Collaboration, G. Arnison *et al.*, *ibid.* **123B**, 115 (1983).
- ²K. Fialkowski and W. Kittel, Rep. Prog. Phys. **46**, 1283 (1983).
- ³E. M. Levin and L. L. Frankfurt, Pis'ma Zh. Eksp. Teor. Fiz. **2**, 105 (1965) [JETP Lett. **2**, 65 (1965)]; H. J. Lipkin and F. Scheck, Phys. Rev. Lett. **16**, 71 (1966).
- ⁴H. Goldberg, Nucl. Phys. **B44**, 149 (1972).
- ⁵W. Ochs, Nucl. Phys. **B118**, 397 (1977).
- ⁶G. Eilam and Y. Gell, Phys. Rev. D **10**, 3634 (1974).
- ⁷Z. Koba, H. B. Nielsen, and P. Olesen, Nucl. Phys. **B40**, 317 (1972).
- ⁸H. M. Georgi, S. L. Glashow, M. E. Machacek, and D. V. Nanopoulos, Ann. Phys. (N.Y.) **114**, 273 (1978); G. L. Kane and Y. P. Yao, Nucl. Phys. **B137**, 313 (1978); Y. Afek, C. Leroy, B. Margolis, and P. Valin, Phys. Rev. Lett. **45**, 85 (1980); T. K. Gaisser and F. Halzen, *ibid.* **54**, 1754 (1985); P. L'Heureux, B. Margolis, and P. Valin, Phys. Rev. D **32**, 1681 (1985).
- ⁹S. S. Gershteyn and A. A. Logunov, Yad. Fiz. **39**, 1514 (1984) [Sov. J. Nucl. Phys. **39**, 960 (1984)].
- ¹⁰A. G. Ekspong, in *Mesons, Isobars, Quarks, and Nuclear Excitations*, proceedings of the International School of Subnuclear Physics, Erice, 1983 [Progress in Particle and Nuclear Physics, edited by D. Wilkinson (Pergamon, London, 1984), Vol. 11].
- ¹¹UA5 Collaboration, R. E. Ansorge, in *Proceedings of HEP83*, International Europhysics Conference on High Energy Physics, Brighton, England, 1983, edited by J. Guy and C. Costain (Rutherford Laboratory, Chilton, 1983), p. 268; Phys. Rep. (to be published).
- ¹²S. Pokorski and S. Wolfram, Z. Phys. C **15**, 111 (1982).
- ¹³R. P. Feynman, *Photon-Hadron Interactions* (Benjamin, New York, 1972), p. 247.
- ¹⁴A. Wroblewski, Acta Phys. Pol. **B4**, 857 (1973).
- ¹⁵S. Rudaz and P. Valin, University of Minnesota Report No. UMN-TH-523/85 (unpublished).
- ¹⁶A. J. Buras, J. Dias de Deus, and R. Moller, Phys. Lett. **47B**, 251 (1973).
- ¹⁷A. M. Polyakov, Zh. Eksp. Teor. Fiz. **60**, 1572 (1971) [Sov. Phys. JETP **33**, 850 (1971)].
- ¹⁸*Higher Transcendental Functions* (Bateman Manuscript Project), Vol. 1, edited by A. Erdélyi (McGraw-Hill, New York, 1953), p. 52.
- ¹⁹V. V. Ammosov *et al.*, Phys. Lett. **42B**, 519 (1972); W. M. Morse *et al.*, Phys. Rev. D **15**, 66 (1977); C. Bromberg *et al.*, Phys. Rev. Lett. **31**, 1563 (1973); S. Barish *et al.*, Phys. Rev. D **9**, 2689 (1974); A. Firestone *et al.*, *ibid.* **10**, 2080 (1974).
- ²⁰E. Eichten, I. Hinchliffe, K. Lane, and C. Quigg, Rev. Mod. Phys. **56**, 579 (1984).
- ²¹G. Pancheri, in *Proceedings of the 15th International Dynamics*, Lund, 1984, edited by G. Gustafson and C. Peterson (World Scientific, Singapore, 1984); P. Carruthers, Los Alamos Report No. LA-UR-84-1084 (unpublished).
- ²²A. Capella and J. Tran Thanh Van, Z. Phys. C **10**, 249 (1981); **18**, 85 (1983).
- ²³W. Bartel and A. N. Diddens, CERN-NP Internal Report No. 73-4, 1973 (unpublished); H. J. Lipkin, Phys. Rev. D **11**, 1827 (1975); U. Amaldi *et al.*, Phys. Lett. **66B**, 390 (1977); M. M. Block and R. N. Cahn, Phys. Lett. **120B**, 224 (1983).
- ²⁴C. Bourrely and A. Martin, in *Proceedings of the CERN Workshop on Large Hadron Collider in the LEP Tunnel*, Lausanne 1984, edited by M. Jacob (CERN Report No. 84-10), Vol. 1, p. 323; A. Martin, in *Proceedings of the Fourth Topical Workshop on Proton-Antiproton Collider Physics*, Bern, 1984, edited by H. Hanni and J. Schacher (CERN Report No. 84-09), p. 308.
- ²⁵M. Froissart, Phys. Rev. **123**, 1053 (1961); A. Martin, *ibid.* **129**, 1432 (1963); Nuovo Cimento **42**, 930 (1966); L. Lukaszuk and A. Martin, *ibid.* **52A**, 122 (1967).
- ²⁶UA4 Collaboration, M. Bozzo *et al.*, Phys. Lett. **147B**, 392 (1984); UA1 Collaboration, G. Arnison *et al.*, *ibid.* **128B**, 336 (1983).
- ²⁷A. Breakstone *et al.*, Phys. Rev. D **30**, 528 (1984).
- ²⁸B. S. Chaudhary and P. K. Malhotra, Nucl. Phys. **B86**, 360 (1975); S. Tasaka *et al.*, Phys. Rev. D **25**, 1765 (1982).
- ²⁹This excludes, for example, the ISR data of Thome *et al.*, Nucl. Phys. **B129**, 365 (1977), which has a clearly increasing trend for the moments C_j with the values at the lower energies being lower than those of Breakstone *et al.* (Ref. 27). This would also be the case for the moments C'_j which would improve the agreement with our theoretical curve.
- ³⁰UA5 Collaboration, G. J. Alner *et al.*, Phys. Lett. **138B**, 304 (1984).
- ³¹C. Conta *et al.*, Nucl. Phys. **B175**, 97 (1980).
- ³²J. Pumplin, Phys. Rev. D **8**, 2899 (1973).